Translational Oncology
www.transonc.com

Volume 10 Number 22 April 2017 pp. 262–270 262

# Multimodality Imaging of Bone Marrow–Derived Dendritic Cell Migration and Antitumor Immunity[1]

**Su-Bi Ahn[*,2], Sang Bong Lee[*,†,2], Thoudam Debraj Singh[*], Sung Jin Cho[†,‡], Sang Kyoon Kim[§], In-Kyu Lee[†,¶], Shin Young Jeong[*], Byeong-Cheol Ahn[*], Jaetae Lee[*,#], Sang-Woo Lee[*,†] and Yong Hyun Jeon[†,§]**

[*]Department of Nuclear Medicine, Kyungpook National University Hospital, Daegu, South Korea; [†]Leading-edge Research Center for Drug Discovery and Development for Diabetes and Metabolic Disease, Kyungpook National University Hospital, Daegu, South Korea; [‡]New Drug Development Center, Daegu-Gyeongbuk Medical Innovation Foundation, Daegu 41061, South Korea; [§]Laboratory Animal Center, Daegu-Gyeongbuk Medical Innovation Foundation, Daegu, Republic of Korea; [¶]Department of Internal Medicine, School of Medicine, Kyungpook National University, Daegu, South Korea; [#]Daegu-Gyeongbuk Medical Innovation Foundation, Daegu, South Korea

## Abstract

Here, we sought to monitor bone marrow–derived dendritic cell (BMDC) migration and antitumor effects using a multimodal reporter imaging strategy in living mice. BMDCs were transduced with retroviral vector harboring human sodium iodide symporter (*hNIS*, nuclear imaging reporter), firefly *luc2* (optical imaging reporter), and *thy1.1* (surrogate marker of *NIS* and *luc2*) genes (BMDC/NF cells). No significant differences in biological functions, including cell proliferation, antigen uptake, phenotype expression, and migration ability, were observed between BMDC and BMDC/NF cells. Combined bioluminescence imaging and I-124 positron emission tomography/computed tomography clearly revealed the migration of BMDC/NF cells to draining popliteal lymph nodes at day 7 postinjection. Interestingly, marked tumor protection was observed in mice immunized with TC-1 lysate-pulsed BMDC/NF cells. Our findings suggested that multimodal reporter gene imaging of NIS and luciferase could provide insights into the biological behaviors of dendritic cells in living organisms and could be a useful tool for the optimization of DC-based immunotherapy protocols.

*Translational Oncology (2017) 10, 262–270*

Address all correspondence to: Sang-Woo Lee, MD, PhD, Department of Nuclear Medicine, Kyungpook National University Hospital, 50 Samduk 2-ga, Daegu, 700-721, South Korea. or Yong Hyun Jeon, PhD, Laboratory Animal Center, Daegu-Gyeongbuk Medical Innovation Foundation (DGMIF), 80. Cheombok-ro. Dong-gu, Daegu, Korea.
E-mail: swnmlee@knu.ac.kr

[1] Funding Sources: This work was supported by National Research Foundation of Korea (NRF) grants funded by the Korea government (MSIP) (nos. NRF-2014R1A4A1071040, 2009-0078222, 2009-0078234, 2014R1A1A1003323, and NRF-2015M2A2A7A01045177); a grant of the Korea Health Technology R&D Project through the Korea Health Industry Development Institute (KHIDI), funded by the Ministry of Health & Welfare (grant number: HI16C1501); the National Nuclear R&D Program through the National Research Foundation of Korea (NRF) funded by the Ministry of Education, Science, and Technology (no. 2012M2A2A7014020); a grant from the Medical Cluster R&D Support Project through the Daegu-Gyengbuk Medical Innovation Foundation (DGMIF), funded by the Ministry of Health & Welfare (grant number: HT13C0002); the BK21 PlusKNU Biomedical Convergence Program, Department of Biomedical Science, Kyungpook National University; a grant of the Korea Health Technology R&D Project through the Korea Health Industry Development Institute (KHIDI), funded by the Ministry of Health & Welfare (grant number: HI15C0001); by a grant of the Medical Cluster R&D support project through the Daegu-Gyeongbuk Medical Innovation Foundation (DGMIF), funded by the Ministry of Health & Welfare, Republic of Korea (grant number: HT15c0003) HT15C0003; and the Radiation Technology R&D program through the National Research Foundation of Korea funded by the Ministry of Science, ICT, & Future Planning (NRF-2012M2A2A7013480).
[2] The first two authors contributed equally to this study.
Received 25 October 2016; Revised 11 January 2017; Accepted 13 January 2017


1936-5233/17
http://dx.doi.org/10.1016/j.tranon.2017.01.003

## Introduction

Bone marrow–derived dendritic cells (BMDCs) are professional antigen-presenting cells that express several specialized molecules, including major histocompatibility complex (MHC) class I/II molecules, costimulatory molecules (B7), and adhesion molecules (intracellular adhesion molecule [ICAM]-1, ICAM-3, and lymphocyte function–associated antigen 3), and that stimulate effectors such as CD4 and CD8 T cells [1–3]. Because of their unique characteristics, BMDCs can recognize various tumor antigenic peptides, including carcinoembryonic antigen and human papilloma virus 16 E6/E7, resulting in strong antitumor immunity [4–6]. Although several cancer therapeutic strategies using DC-based immunotherapy alone or in combination with radiation therapy and chemotherapy have been developed, these treatments are only partially effective because there are currently no techniques to monitor the biological behaviors of DCs *in vivo*. Therefore, to optimize DC-based immunotherapy strategies, it is necessary to develop reliable and quantitative imaging tools that enable monitoring the localization, distribution, and migration of infused DCs *in vivo*.

Molecular imaging with reporter genes to observe the proliferation, localization, and migration of cancer cells, stem cells, and immune cells has been widely investigated [7–9]. *In vivo* bioluminescent imaging (BLI) with firefly and Renilla luciferases has multiple advantages, such as high sensitivity, ease of use, cost-effectiveness, and no requirement for complex facilities. However, BLI is associated with limited tissue penetration depth; thus, it is difficult to detect cells of interest in deep tissues. Nuclear medicine imaging of sodium iodide symporter (*NIS)* and herpes simplex virus type 1 thymidine kinase (*HSV1-tk*) gene expression has great sensitivity and no depth limitation; however, this method cannot be used to distinguish small populations of cells located at a specific site of interest because of high background activity resulting from physiological tracer uptake by surrounding tissue. To overcome these limitations of single imaging modalities, researchers have attempted to develop multimodal reporter gene imaging strategies that can be used for tracking early distribution and migration of cells in deep tissues [10–14].

In this study, we attempted to visualize the migration of primary BMDCs to lymphoid organs, particularly draining lymph nodes, using a multimodal reporter gene system involving *NIS* and *luc2* genes in living mice. Furthermore, we extensively investigated the antitumor immunity induced by vaccination of mice grafted with TC-1 cancer cells expressing *Renilla luciferase* with BMDCs expressing the multimodal reporter, an important concept in the clinical application of multimodal reporter systems.

## Materials and Methods

### *Ethics Statement*

All described procedures were reviewed and approved by Kyungpook National University (KNU-2012-43) Animal Care and Use Committee and performed in accordance with the Guiding Principles for the Care and Use of Laboratory Animals.

### *Transduction of Multimodal Reporter Genes into BMDCs*

A retroviral vector harboring *hNIS*, firefly *luc2*, and *Thy1.1* genes termed "Retro-NFT" was established by CosmoGenetech Co. Ltd. (Seoul, South Korea) using a pCHAC backbone (Allele Biotechnology, San Diego, CA). Each reporter gene was linked with a T2A sequence to allow effective and independent reporter expression (Figure 1*A*).

Gryphon packaging cells (Allele Biotechnology, San Diego, CA) were cultured in Dulbecco's modified Eagle's medium (Life Technologies, Grand Island, NY) with 10% FBS. Ecotropic retrovirus particles were generated by transfecting the Gryphon cells with Retro-NFT using a calcium phosphate transfection kit (Invitrogen, Carlsbad, CA). Three days later, fresh viral supernatant was used for spin infection (2000 rpm, 90 minutes, 32°C) of BMDCs, and infected cells were plated in 100-mm Petri dishes containing complete medium. BMDCs expressing Retro-NFT are hereafter referred to as "BMDC/NF cells." After staining of the cells with an APC-Cy7–conjugated Thy1.1 antibody (BD Biosciences, San Jose, CA), Thy1.1-positive cells were determined using a BD Accuri C6 flow cytometer (BD Biosciences).

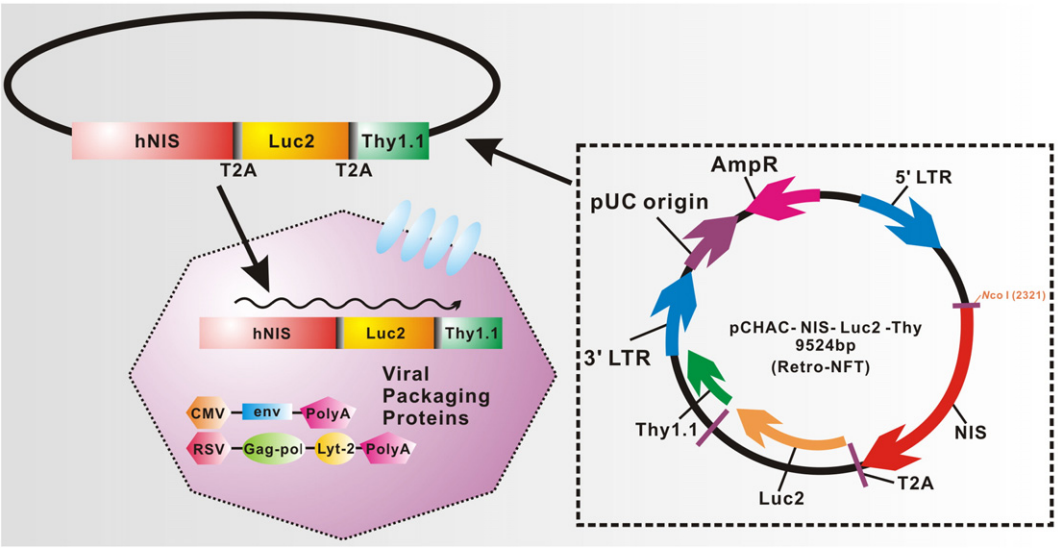


**Figure 1.** Schematic representation of the principle and multimodal reporter gene construct for *in vivo* tracking of DCs. The multimodal reporter system involves expression of the *hNIS, luc2,* and *Thy1.1* genes, which act as a nuclear reporter, optical reporter, and surrogate for *hNIS* and *luc2*, respectively.

### *Reporter Gene Assay*

For I-125 uptake assays, the indicated number of cells was plated in 24-well plates. One day after seeding, the cells were incubated with 500 μl of Hank's balanced salt solution (HBSS, HyClone, Logan, UT, USA) containing 0.5% bovine serum albumin (bHBSS), 3.7 kBq carrier-free I-125 (PerkinElmer), and 10 μM sodium iodide (specific activity 740 MBq/mmol) at 37°C for 30 minutes. After incubation, the cells were washed twice as quickly as possible with ice-cold bHBSS buffer and lysed in 500 μl of 2% sodium dodecyl sulfate. Radioactivity was measured using a Packard Cobra II gamma-counter (PerkinElmer, Waltham, MA).

For luciferase assays, cells were plated in white and clear-bottom 96-well plates. The appropriate substrate was added to each well 24 hours later, and BLI signals were measured using a microplate reader (BMG Labtech, Offenburg, Germany) or IVIS Lumina III (PerkinElmer).

### *Proliferation Assay*

Cell proliferation was assayed using a Cell Counting Kit (CCK)-8 (Dojindo Laboratories, Tokyo, Japan). BMDCs and BMDC/NF cells were plated at $1 \times 10^4$ cells per well in 96-well plates. Ten microliters of CCK-8 solution was added to each well at 24 and 48 hours after cell seeding, after which the plates were incubated at 37°C for 3 hours. The absorbance at 450 nm was measured using a microplate reader (BMG Labtech).

### *Flow-Cytometric Analysis*

BMDCs and BMDC/NF cells were stained with PE-conjugated anti-CD54, anti-CD86, anti–H-2Kb (MHC class I,) or anti–I-A/I-E (MHC class II); FITC-conjugated anti-CD11c; or APC-Cy7–conjugated anti-CD197 (CCR-7) antibodies (BD Biosciences) at 4°C for 30 minutes. After washing with PBS, the cells were analyzed using a BD Accuri C6 flow cytometer. Isotype-matched monoclonal antibodies were used as controls. The data were analyzed using the FlowJo analysis software (FlowJo, Ashland, OR).

### *Transwell Migration Assay*

BMDCs and BMDC/NF cells were incubated with 1.0 μg/ml of prostaglandin $E_2$ ($PGE_2$; Sigma-Aldrich, St. Louis, MO) for 24 hours. Then, culture medium containing CCL19 (PeproTech, Rocky Hill, NJ) was added to the lower chamber, and $2 \times 10^5$ cells were added to the upper chamber, which contained polycarbonate membranes with 5-μm pores (BD Biosciences). After a 2-hour incubation at 37°C, the migrated cells were collected and counted by flow cytometry. Events acquired for 60 seconds were analyzed using FlowJo.

### *Antigen Uptake Efficiency*

BMDCs and BMDC/NF cells were incubated with 100 μg/ml of Texas Red–ovalbumin (Life Technologies) at 4°C or 37°C for 1 hour. After labeling, the cells were washed with PBS and analyzed using a BD Accuri C6 flow cytometer.

### *In Vivo Therapy*

The scheme for *in vivo* therapy is outlined in Figure S2. Total lysates of TC-1/Rluc cells were prepared by freezing and thawing thrice. Fifty micrograms of each lysate was incubated with $2 \times 10^6$ BMDC/NF cells overnight, and pulsed or unpulsed BMDC/NF cells were intramuscularly injected into the hind legs of mice once a week for 2 weeks ($n = 7$ mice/group). After the last immunization, the mice were challenged with TC-1/luciferase, and tumor progression was monitored with BLI. After imaging, the mice were sacrificed. The tumors were excised, and the tumor weights were measured.

### *In Vivo Imaging of DC Migration to Lymph Nodes*

Mice ($n = 5$) received 30 ng TNF-α *via* subcutaneous injection into the hind footpads. One day later, $1 \times 10^6$ BMDCs and BMDC/NF cells were subcutaneously injected into the left and right footpads of the hind leg, respectively, and combined optical and positron emission tomography (PET)/computed tomography (CT) imaging was performed at the indicated times.

After imaging, the mice were sacrificed. The DPLNs and control popliteal lymph nodes were excised, placed on a black sheet, and subjected to BLI *ex vivo*.

### *Cytotoxic T Lymphocyte (CTL) Assay*

Splenocytes harvested from tumor-bearing mice were restimulated with total TC-1 lysates and interleukin (IL)-2 for 4 days. Then, the cells were washed twice with PBS. TC-1/Rluc cells were used as target cells. Target cells were seeded in black, clear-bottomed 96-well plates ($1 \times 10^4$ cells/well). After overnight incubation, splenocytes were added as effectors to the wells at an effector/target ratio of 5:1. Eleven hours later, luciferase activity was measured with an IVIS Lumina III instrument (PerkinElmer).

### *Statistical Analysis*

All data are expressed as the mean ± standard deviation (SD) from at least three representative experiments, and statistical significance was determined using an unpaired Student's *t* test with GraphPad Prism 5. $P$ values $< .05$ were considered statistically significant.

## Results and Discussion

### *Design of the Retro-NFT Multimodal Reporter System Harboring hNIS, luc2, and Thy1.1*

For *in vivo* DC tracking, we designed a new multimodal reporter system, Retro-NFT, based on a retroviral vector harboring NIS as a nuclear imaging reporter, firefly luc2 as an optical reporter, and Thy1.1 as a surrogate marker for NIS and luc2 (Figure 1). For effective protein expression, each reporter gene was linked with self-cleaving 2A peptides, which allow for highly efficient cleavage.

### *Evaluation of the Retro-NFT Multimodal Reporter System in Gryphon E Cells*

After transfection of Gryphon E cells with Retro-NFT, we could detect mRNA expression of the respective reporters by reverse transcription polymerase chain reaction analysis (data not shown). Fluorescence-activated cell sorting analysis with anti-Thy1.1 revealed Thy1.1 protein expression in 90.8% of Retro-NFT–transfected cells (Figure 2*A*). Furthermore, there was an increase in iodide uptake in transfected but not parental cells (Figure 2*B*). Luciferase assays showed a cell number–dependent increase in signal in transfected but not parental cells (Figure 2*C*).

### *Introduction of the Multimodal Reporter Genes into BMDCs*

On day 3 posttransduction of BMDCs to generate BMCD/NF cells, significant Thy1.1 protein expression was detected in 18.2% of the cells (Figure 3*A*). Because *Thy1.1* acted as a surrogate marker for *hNIS* and *luc2*, the population expressing *Thy1.1* indirectly represented *hNIS*- and *luc2*-positive BMDC/NF cells. Immunoblotting with anti-NIS and anti-luc2 antibodies showed specific bands

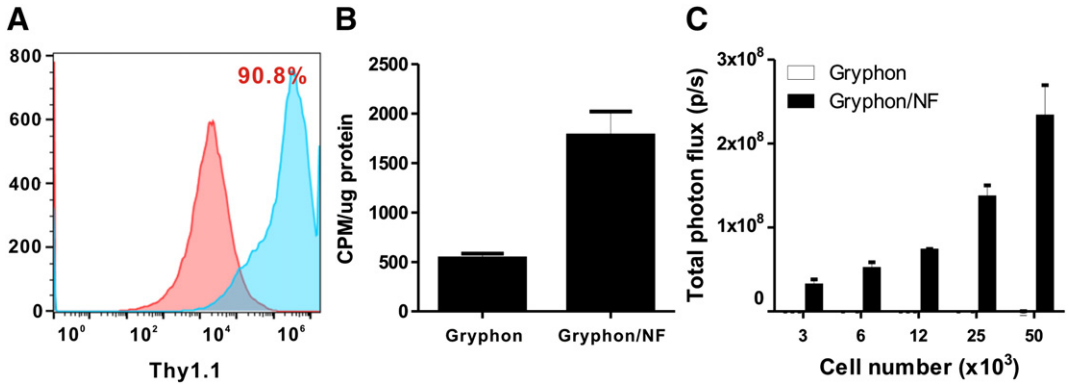


**Figure 2.** Expression characteristics of the multimodal reporter gene system for *in vivo* tracking of DCs. The multimodal retroviral vector construct was transfected into virus-producing Gryphon E cells, and the expression of each protein was determined by (A) fluorescence-activated cell sorting analysis with anti-Thy1.1 antibodies (red: isotype-matched cells, blue: anti-Thy1.1-stained cells), (B) iodide uptake for NIS, and (C) luciferase assays in 293FT and 293FT/NFT cells. Data indicate means ± SDs.

corresponding to the respective reporters in BMDC/NF cells but not in BMDCs (Figure 3*B*).

Next, we examined hNIS and luc2 protein activity by iodide uptake assays and *in vitro* BLI. As shown in Figure 3*C*, iodide uptake was increased by five-fold in BMDC/NF cells, whereas the increase was completely inhibited by treatment with the NIS inhibitor $KClO_4$. *In vitro* BLI revealed that the luciferase signal was increased in a cell number–dependent manner in BMDC/NF cells but not in BMDCs (Figure 3*D*).

Next, we determined whether the radioactive and optical signals from reporter BMDCs correlated with the number of injected reporter BMDCs in mice. As shown in Figure 4*A*, BLI and radioactive signals increased in a cell number–dependent manner following subcutaneous injection. A good correlation ($r^2$ = 0.8618

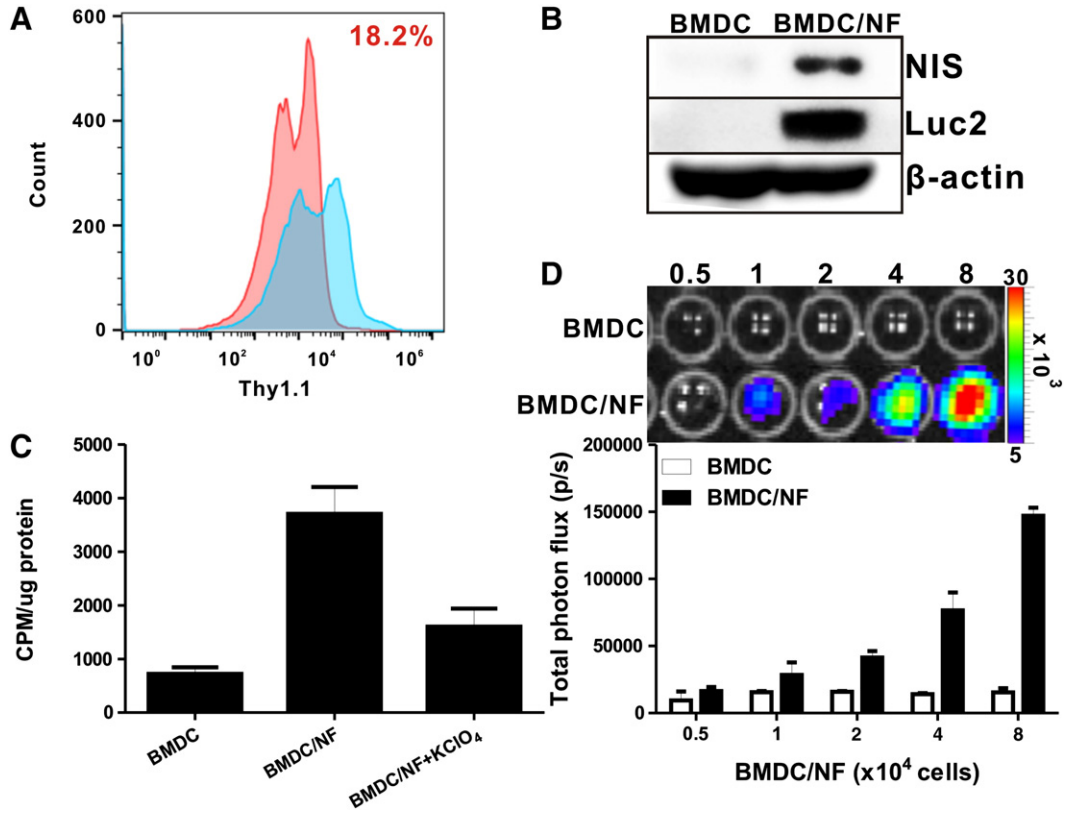


**Figure 3.** Expression of the multimodal reporter by primary BMDCs. (A) Flow-cytometric analysis of BMDC/NF cells using anti-Thy1.1 antibodies (red: isotype-matched cells, blue: anti-Thy1.1–stained cells). (B) Immunoblot analysis of hNIS and luc2 protein expression with anti-NIS or anti-luciferase antibodies, (C) iodide uptake ($KClO_4$ as an NIS inhibitor), and (D) *in vitro* BLI in BMDCs and BMDC/NF cells. Experiments were performed at least in triplicate, and bar graphs represent means ± SDs.

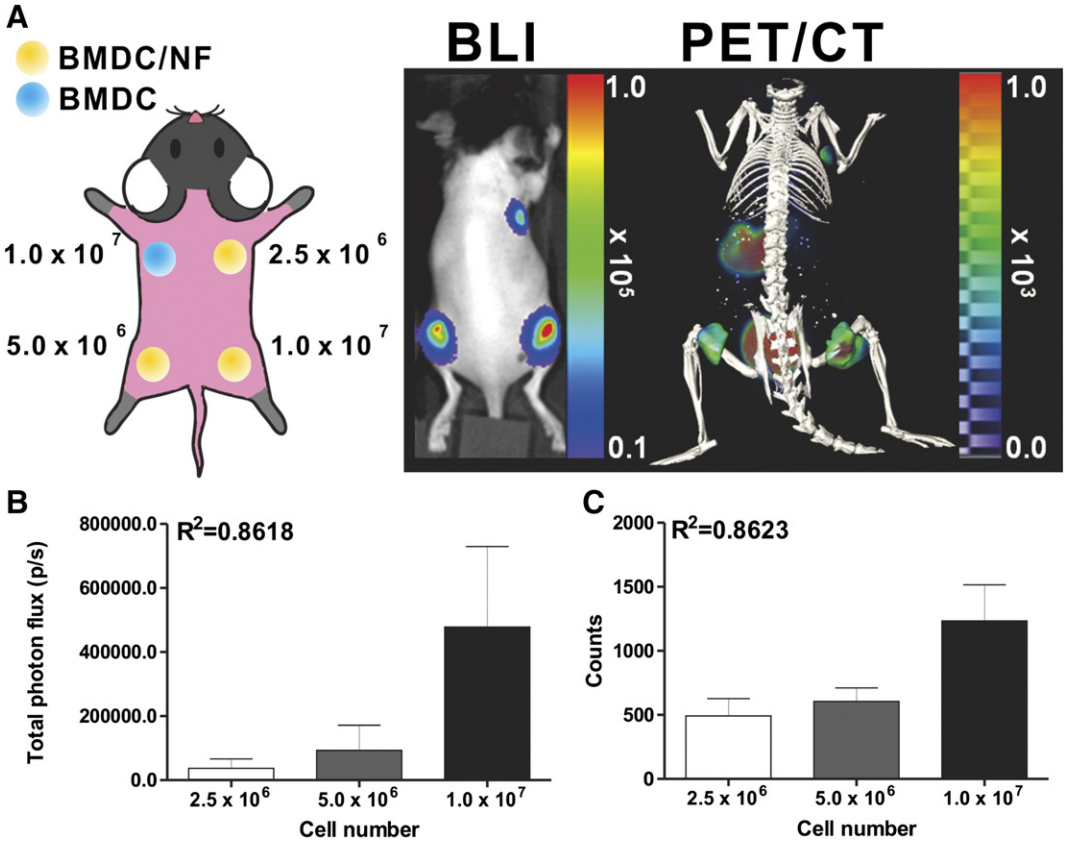


**Figure 4.** Visualization of BMDC/NF cells following subcutaneous injection. (A) BLI and I-124 PET/CT imaging of different numbers of subcutaneously injected BMDCs or BMDC/NF cells. (B) Correlation between the number of injected BMDC/NF cells and BLI or radioactive signal. Bar graphs represent means ± SDs.

and 0.8623 for BLI and PET imaging, respectively) was observed between the number of DCs and BLI and radioactive signals from reporter BMDCs (Figure 4, *B* and *C*).

### *Effects of Multimodal Reporter Genes on Biological Function of BMDCs*

Molecular imaging with reporter genes has been used to track circulating cancer cells and to determine the biological behaviors of immune and stem cells in living mice [7,9,15–18]. For successful application of reporter genes to DC tracking *in vivo*, the reporter should not induce adverse effects on cell proliferation or biological functions.

To this end, we first compared proliferation between parental BMDCs and BMDC/NF cells. CCK-8 assays indicated no significant differences between the two groups (Figure 5*A*). Next, we investigated the effects of reporter construct introduction on antigen uptake, phenotype marker expression, and Transwell migration of DCs. The results showed no differences in uptake of the OVA peptide at 37°C between groups; however, antigen uptake at 4°C was markedly inhibited in both groups (Figure 5*B*). Phenotypic analysis demonstrated no significant differences in the expression of the DC-specific markers CD11c, CD54, CD86, MHC class I and II, and CCR7 between BMDCs and BMDC/NF cells (Figure 5*C*). In Transwell migration assays, there was a distinct increase in the migration of BMDCs in the presence of $PGE_2$, which has been shown to upregulate the expression of CCR7 in DCs and may increase the responsiveness of DCs to C-C chemokine ligands [19], with no difference between BMDCs and BMDC/NF cells (Figure 5*D*).

These results indicated that the introduction of the multimodal reporter genes did not induce adverse effects on biological functions of BMDCs.

### *In Vivo Imaging of BMDC Migration with the Multimodal Reporter*

DCs are routinely administered *via* intramuscular, intravenous, and intradermal routes for DC vaccination [20–24]. It is important to determine whether infused DCs are successfully delivered to the target site for effective generation of antitumor immunity. Therefore, we attempted to track BMDC migration by multimodal reporter gene imaging following subcutaneous injection into the footpads of mice. Several studies have reported that small populations of DCs migrate to the draining lymph nodes, such as popliteal lymph nodes and inguinal lymph nodes, after subcutaneous injection into the footpads of mice [25,26]. The administration of immune effectors can lead to nonspecific accumulation of radioiodine at the injection site through an immune cell–mediated inflammatory reaction. Therefore, BMDC-injected footpads were included as a control (Figure S1). It has been demonstrated that preexposure of the injection site to proinflammatory cytokines such as TNF-α results in enhanced DC migration to draining lymph nodes [27]. Therefore, in this study, mice received 30 ng TNF-α *via* subcutaneous injection into the hind footpads.

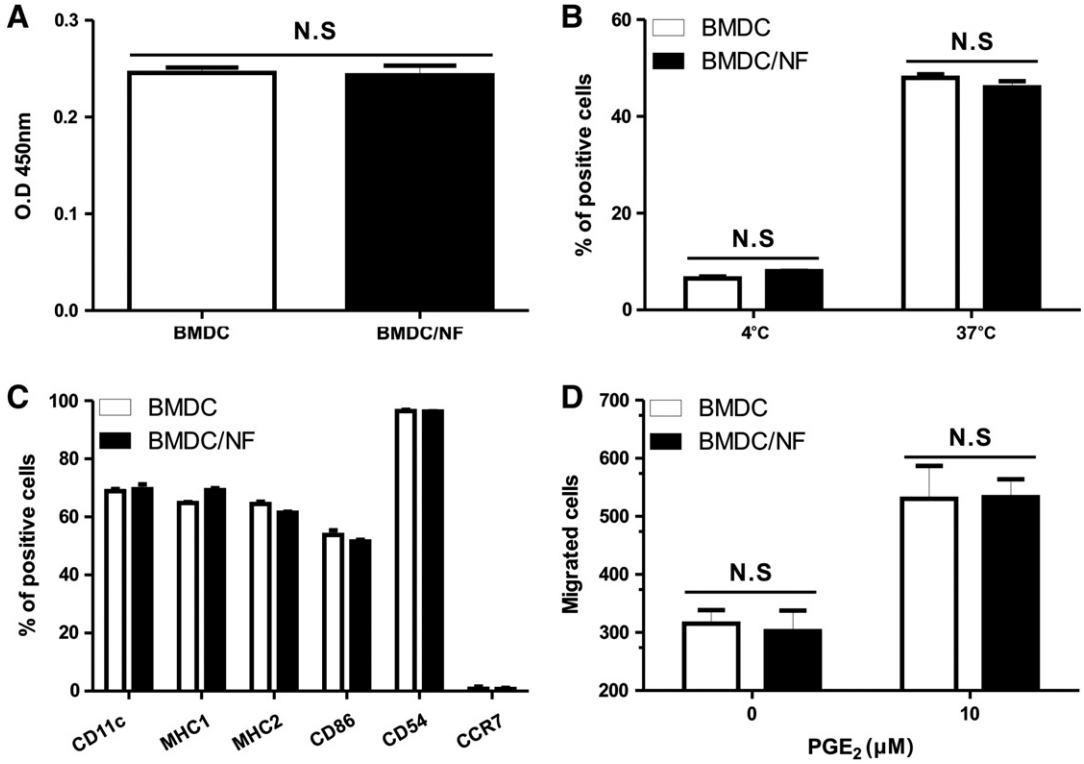


**Figure 5.** Effects of multimodal reporter expression on biological functions of BMDCs. (A) Cell proliferation assay with CCK-8 reagents; (B) antigen uptake assay with Texas Red–ovalbumin; (C) phenotypic marker expression analyzed using specific antibodies; and (D) Transwell migration assay for BMDCs and BMDC/NF cells. Experiments were performed at least in triplicate, and bar graphs represent means ± SDs. N.S. = not significant.

After injection of BMDC/NF cells, we monitored their migration with combined I-124 PET/CT and BLI on days 0 and 7 (Figure S1). On day 0 postinjection, intense BLI signals were detected in BMDC/NF-injected but not BMDC-injected footpads (Figure 6*A*, *upper panel, red arrow*). Consistent herewith, intense radioactive signals were observed only in BMDC/NF-injected footpads (Figure 6*A, bottom panel, red arrow*). We did not observe migrated BMDCs in DPLNs on day 0. However, on day 7 postinjection, *in vivo* BLI clearly showed migrated BMDCs in DPLNs (Figure 6*A, upper panel, yellow arrow*). Consistent herewith, *in vivo* PET/CT with I-124 revealed intense radioiodine signal in DPLNs (Figure 6*A, bottom panel, yellow arrow*). However, no BLI and radioactive signals were detected in BMDC-injected footpads. The BLI signal in DPLNs ranged from $1.04 \times 10^5$ P/cm$^2$/s/sr to $5.62 \times 10^5$ P/cm$^2$/s/sr (Figure 6*B*). There was a relative increase in radioiodine uptake by DPLNs from 17.4% to 38.2% (Figure 6*C*).

To identify the BMDCs that had migrated to DPLNs, the mice were sacrificed, and DPLNs were excised for *ex vivo* imaging and immunoblotting with anti-hNIS and anti-luc2 antibodies. *Ex vivo* imaging with combined BLI and PET/CT demonstrated strong signals in DPLNs but not control popliteal lymph nodes (Figure 6*D*), and protein expression of both hNIS and luc2 was detected in DPLNs of BMDC/NF- but not BMDC-injected footpads (Figure 6*E*).

These results suggested that multimodal reporter imaging with *hNIS* and *luc2* genes is feasible for monitoring the migration of primary BMDCs to draining lymph nodes in living mice.

### *Application of Multimodal Reporter Gene Imaging in the Experimental Setting of DC-Based Immunotherapy*

We investigated whether injection with BMDC/NF cells could successfully generate antitumor immunity in immunocompetent mice. For this experiment, we selected the mouse cervical cancer cell line TC-1 expressing E7 antigen. This model has been used to evaluate the antitumor immune response generated by DNA or DC vaccines expressing the E7 antigen [20,28,29]. To visualize the antitumor effects *in vivo*, we further engineered the TC-1 cells to express *Rluc*. Because Rluc uses the substrate coelenterazine, which is different from the firefly luciferase luc2 substrate, reporter BMDCs and tumor cell proliferation could be monitored simultaneously *in vivo*.

BMDC/NF cells were pulsed with TC-1 lysates, and mice were immunized with pulsed BMDC/NF cells once a week for 2 weeks (Figure S2). After the first intramuscular injection of pulsed BMDC/NF cells, we examined whether the cells were successfully transferred to the vaccination site using PET/CT and BLI. As shown in Figure 7*A*, distinct radioactive and BLI signals were detected at the injection site for both pulsed and unpulsed BMDC/NF cells, indicating successful delivery of BMDC/NF cells to the vaccination site, which is critical for the effective generation of an antitumor immune response. Similarly, we observed radioactive and BLI signals at the injection site following the second vaccination (data not shown).

After the final vaccination, the mice were challenged with TC-1/Rluc, and tumor progression was monitored with BLI (Figure S2). Until day 7 postchallenge, there were no significant differences in

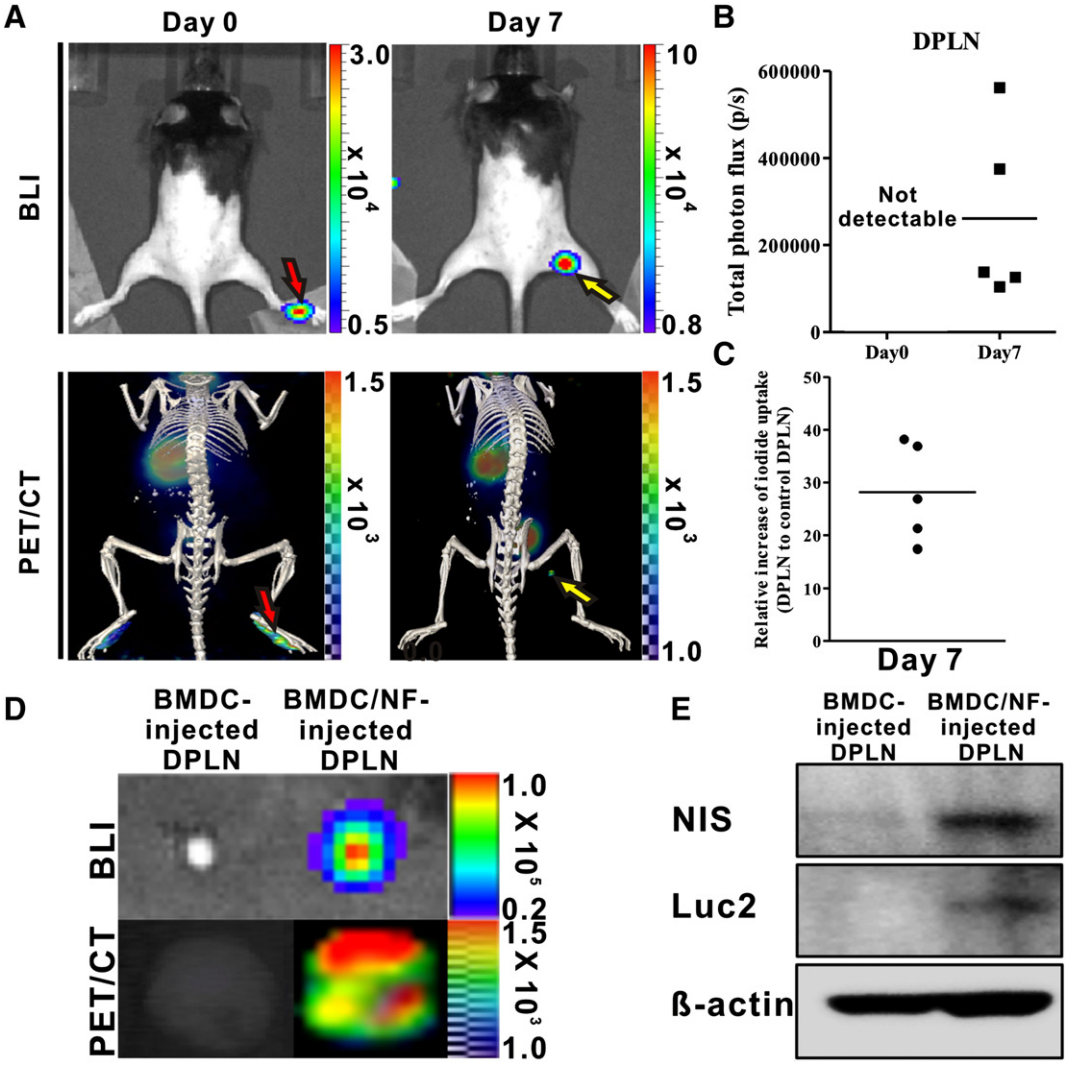


**Figure 6.** *In vivo* imaging of BMDC migration with the multimodal reporter construct in living mice. (A) Combined BLI (upper) and PET/CT (bottom) of the migration of BMDC/NF cells to DPLNs at days 0 and 7 postinjection. Red and yellow arrows indicate the injected site and draining popliteal lymph nodes, respectively. (B, C) Quantification of BLI and radioactive signals in footpads and DPLNs. (D) *Ex vivo* BLI and PET/CT of excised control popliteal lymph nodes (PLNs, left) and DPLNs (right). (E) Immunoblot analysis of excised DPLNs and control PLNs with anti-NIS and anti-luciferase antibodies to evaluate the presence of migrated BMDC/NF cells in DPLNs. Each group consisted of five mice, and experiments were performed at least in triplicate.

tumor-derived BLI signals between pulsed and unpulsed BMDC/NF groups (Figure 7*C*). From day 11, we observed marked tumor protection in mice immunized with pulsed BMDC/NF cells and a higher BLI signal in mice immunized with unpulsed BMDC/NF cells ($P < .05$). The BLI activity values were $2.3 \times 10^{10} \pm 9.8 \times 10^{9}$ P/cm$^2$/s/sr and $1.2 \times 10^{10} \pm 7.1 \times 10^{9}$ P/cm$^2$/s/sr in mice receiving unpulsed and pulsed BMDC/NF cells, respectively (Figure 7*C*). Significant tumor protection was observed in the group immunized with pulsed BMDC/NF cells until 14 days (Figure 7*B*), and excised tumors were smaller and weighed less in the pulsed BMDC/NF–receiving group than in the unpulsed BMDC/NF–receiving group (Figure 7*D*). During the experiment, we did not see any adverse effects of the therapy on body weight or fur appearance in both groups (data not shown).

To explore the immune responses in tumor-bearing mice further, we prepared splenocytes from each group to measure the killing activity of CTLs [28]. We monitored the BLI activity of TC-1/Rluc cells at an effector to target ratio of 5:1 to examine the killing activity of CTLs against TC-1 cells. As shown in Figure 7*E*, the BLI activity in splenocytes from mice immunized with pulsed BMDC/NF cells was lower than that in splenocytes from mice immunized with unpulsed BMDC/NF cells ($P < .05$).

Taken together, these results suggested that the multimodal reporter construct did not adversely affect the generation of antitumor immunity by BMDCs, while facilitating the monitoring of successful delivery following DC vaccination.

## Conclusion

In summary, we developed a new multimodal reporter system, Retro-NFT, suitable for *in vivo* DC tracking, which allowed successful introduction of multiple reporter genes into primary BMDCs *via* retrovirus transduction. Retro-NFT introduction did not have adverse effects on the biological functions of these cells. Furthermore, we could monitor the migration of BMDCs in living

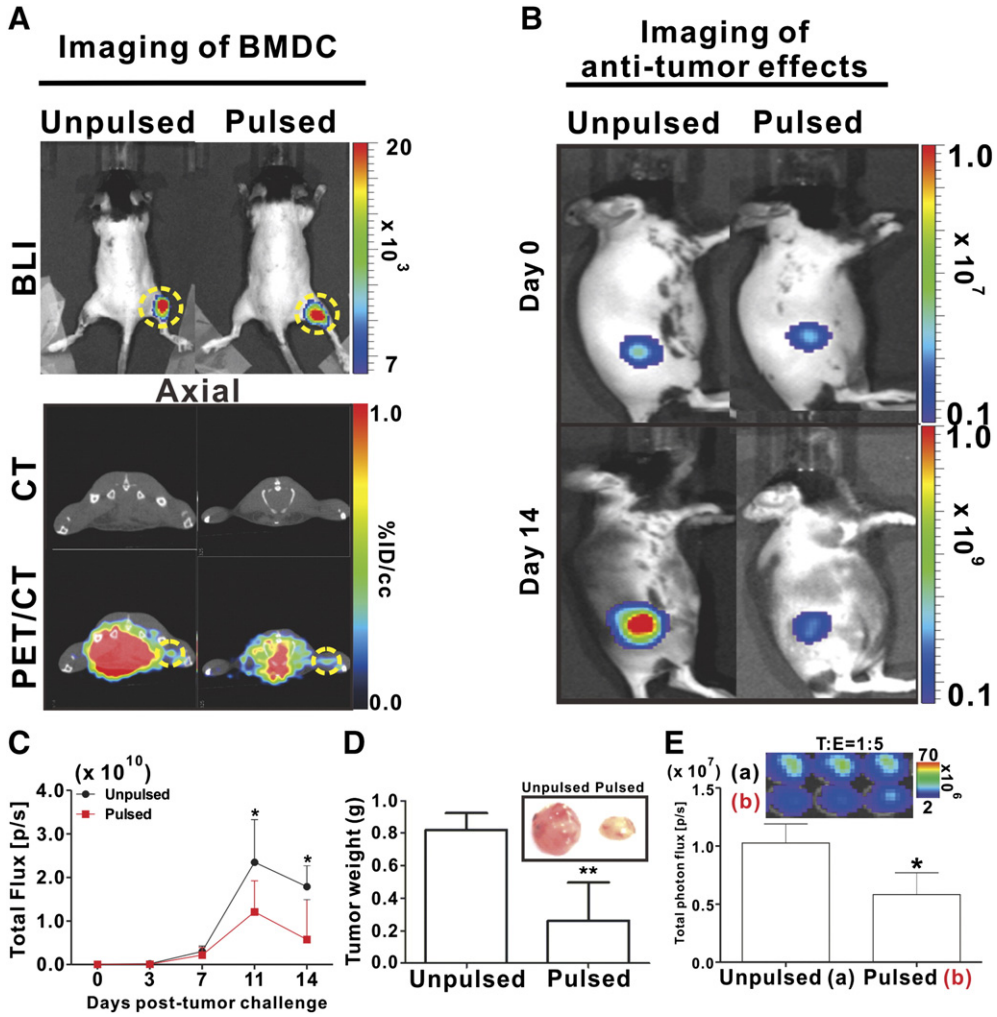


**Figure 7.** Evaluation of antitumor immunity induction by BMDC/NF cells in a cervical cancer model by multimodal reporter gene imaging. (A) *In vivo* BLI and axial PET/CT imaging of unpulsed BMDC/NF cells (left) and pulsed BMDC/NF cells (right) following intramuscular injection. (B) *In vivo* visualization of the antitumor effects of pulsed BMDC/NF cells with *Rluc* reporter gene imaging. Significant tumor protection was observed in mice immunized with pulsed BMDCs. (C) Quantification of the BLI signal in tumors. (D) Measurement of tumor weight; inset: photograph of excised tumor from each group. (E) *In vitro* BLI imaging of the killing activity of CTLs against TC-1/*Rluc* ([a] splenocytes from mice immunized with unpulsed BMDCs, [b] splenocytes from mice immunized with pulsed BMDCs). Each group consisted of seven mice, and experiments were performed at least in triplicate. Values indicate means ± SDs.

mice by employing a combination of BLI and I-124 PET/CT. Importantly, BMDCs expressing the reporter genes could generate antitumor immunity against cervical cancer. Taken together, these results highlight the potential of our multimodal reporter gene system for application as a new imaging platform to evaluate the biological behaviors of BMDCs and to optimize DC-based immunotherapies. However, because the efficiency of viral infection of BMDCs was rather low, it was difficult to detect the early migration of BMDCs to the lymphoid organs. Therefore, it will be necessary to enhance the transfection efficiency of multimodal reporter genes in BMDCs.

## Notes

The authors declare no competing financial interest.

## Appendix A. Supplementary data

Supplementary data to this article can be found online at http://dx.doi.org/10.1016/j.tranon.2017.01.003.

## References

[1] Banchereau J and Steinman RM (1998). Dendritic cells and the control of immunity. *Nature* **392**, 245–252.
[2] Cella M, Sallusto F, and Lanzavecchia A (1997). Origin, maturation and antigen presenting function of dendritic cells. *Curr Opin Immunol* **9**, 10–16.
[3] Steinman RM (1991). The dendritic cell system and its role in immunogenicity. *Annu Rev Immunol* **9**, 271–296.
[4] Ardavín C, Amigorena S, and Reis e Sousa C (2004). Dendritic cells: immunobiology and cancer immunotherapy. *Immunity* **20**, 17–23.
[5] O'Neill DW, Adams S, and Bhardwaj N (2004). Manipulating dendritic cell biology for the active immunotherapy of cancer. *Blood* **104**, 2235–2246.
[6] Cerundolo V, Hermans IF, and Salio M (2004). Dendritic cells: a journey from laboratory to clinic. *Nat Immunol* **5**, 7–10.
[7] Kang JH and Chung JK (2008). Molecular-genetic imaging based on reporter gene expression. *J Nucl Med* **49**(Suppl. 2), 164S–179S.
[8] Gambhir SS (2002). Molecular imaging of cancer with positron emission tomography. *Nat Rev Cancer* **2**, 683–693.
[9] Massoud TF and Gambhir SS (2003). Molecular imaging in living subjects: seeing fundamental biological processes in a new light. *Genes Dev* **17**, 545–580.

[10] Ray P, De A, Min JJ, Tsien RY, and Gambhir SS (2004). Imaging tri-fusion multimodality reporter gene expression in living subjects. *Cancer Res* **64**, 1323–1330.
[11] Ray P, Tsien R, and Gambhir SS (2007). Construction and validation of improved triple fusion reporter gene vectors for molecular imaging of living subjects. *Cancer Res* **67**, 3085–3093.
[12] Culver J, Akers W, and Achilefu S (2008). Multimodality molecular imaging with combined optical and SPECT/PET modalities. *J Nucl Med* **49**, 169–172.
[13] Ponomarev V, Doubrovin M, Serganova I, Vider J, Shavrin A, Beresten T, Ivanova A, Ageyeva L, Tourkova V, and Balatoni J, et al (2004). A novel triple-modality reporter gene for whole-body fluorescent, bioluminescent, and nuclear noninvasive imaging. *Eur J Nucl Med Mol Imaging* **31**, 740–751.
[14] Lee HW, Jeon YH, Hwang MH, Kim JE, Park TI, Ha JH, Lee SW, Ahn BC, and Lee J (2013). Dual reporter gene imaging for tracking macrophage migration using the human sodium iodide symporter and an enhanced firefly luciferase in a murine inflammation model. *Mol Imaging Biol* **15**, 703–712.
[15] Seo JH, Jeon YH, Lee YJ, Yoon GS, Won DI, Ha JH, Jeong SY, Lee SW, Ahn BC, and Lee J (2010). Trafficking macrophage migration using reporter gene imaging with human sodium iodide symporter in animal models of inflammation. *J Nucl Med* **51**, 1637–1643.
[16] Schumacher TN, Gerlach C, and van Heijst JW (2010). Mapping the life histories of T cells. *Nat Rev Immunol* **10**, 621–631.
[17] Ahrens ET and Bulte JWM (2013). Tracking immune cells in vivo using magnetic resonance imaging. *Nat Rev Immunol* **13**, 755–763.
[18] Negrin RS and Contag CH (2006). Innovation — in vivo imaging using bioluminescence: a tool for probing graft-versus-host disease. *Nat Rev Immunol* **6**, 484-U482.
[19] Scandella E, Men Y, Gillessen S, Förster R, and Groettrup M (2002). Prostaglandin E2 is a key factor for CCR7 surface expression and migration of monocyte-derived dendritic cells. *Blood* **100**, 1354–1361.
[20] Wang TL, Ling M, Shih IM, Pham T, Pai SI, Lu Z, Kurman RJ, Pardoll DM, and Wu TC (2000). Intramuscular administration of E7-transfected dendritic cells generates the most potent E7-specific anti-tumor immunity. *Gene Ther* **7**, 726–733.
[21] Jefford M, Maraskovsky E, Cebon J, and Davis I (2001). The use of dendritic cells in cancer therapy. *Lancet Oncol* **2**, 343–353.
[22] Nestle FO, Banchereau J, and Hart D (2001). Dendritic cells: on the move from bench to bedside. *Nat Med* **7**, 761–765.
[23] Kastenmüller W, Kastenmüller K, Kurts C, and Seder RA (2014). Dendritic cell–targeted vaccines —hope or hype? *Nat Rev Immunol* **14**, 705–711.
[24] Figdor CG, de Vries IJ, Lesterhuis WJ, and Melief CJ (2004). Dendritic cell immunotherapy: mapping the way. *Nat Med* **10**, 475–480.
[25] Cho NH, Cheong TC, Min JH, Wu JH, Lee SJ, Kim D, Yang JS, Kim S, Kim YK, and Seong SY (2011). A multifunctional core-shell nanoparticle for dendritic cell–based cancer immunotherapy. *Nat Nanotechnol* **6**, 675–682.
[26] Noh YW, Lim YT, and Chung BH (2008). Noninvasive imaging of dendritic cell migration into lymph nodes using near-infrared fluorescent semiconductor nanocrystals. *FASEB J* **22**, 3908–3918.
[27] Martin-Fontecha A, Sebastiani S, Hopken UE, Uguccioni M, Lipp M, Lanzavecchia A, and Sallusto F (2003). Regulation of dendritic cell migration to the draining lymph node: Impact on T lymphocyte traffic and priming. *J Exp Med* **198**, 615–621.
[28] Cheng WF, Hung CF, Chai CY, Hsu KF, He L, Ling M, and Wu TC (2001). Tumor-specific immunity and antiangiogenesis generated by a DNA vaccine encoding calreticulin linked to a tumor antigen. *J Clin Invest* **108**, 669–678.
[29] Hsieh CY, Chen CA, Huang CY, Chang MC, Lee CN, Su YN, and Cheng WF (2007). IL-6-encoding tumor antigen generates potent cancer immunotherapy through antigen processing and anti-apoptotic pathways. *Mol Ther* **15**, 1890–1897.